THE JOURNAL OF BIOLOGICAL CHEMISTRY VOL. 288, NO. 38, pp. 27220–27231, September 20, 2013

Redox-regulated Cargo Binding and Release by the Peroxisomal Targeting Signal Receptor, Pex5*

Received for publication, June 17, 2013, and in revised form, July 29, 2013 Published, JBC Papers in Press, July 31, 2013, DOI 10.1074/jbc.M113.492694

Changle Ma[1], **Danielle Hagstrom, Soumi Guha Polley, and Suresh Subramani**[2]

From the Section of Molecular Biology, Division of Biological Sciences, University California, San Diego, La Jolla, California 92093-0322

Background: Pex5 transports PTS1 proteins to peroxisomes, releases them there, and returns to the cytosol.
Results: Several steps of the import cycle are controlled by redox-sensitive oligomeric states of Pex5.
Conclusion: Cargo release from Pex5 is achieved by a redox-regulated oligomer to dimer transition of Pex5 and aided by Pex8.
Significance: This redox regulation of Pex5 function provides the first mechanistic view of cargo release.

In its role as a mobile receptor for peroxisomal matrix cargo containing a peroxisomal targeting signal called PTS1, the protein Pex5 shuttles between the cytosol and the peroxisome lumen. Pex5 binds PTS1 proteins in the cytosol via its C-terminal tetratricopeptide domains and delivers them to the peroxisome lumen, where the receptor·cargo complex dissociates. The cargo-free receptor is exported to the cytosol for another round of import. How cargo release and receptor recycling are regulated is poorly understood. We found that Pex5 functions as a dimer/oligomer and that its protein interactions with itself (homo-oligomeric) and with Pex8 (hetero-oligomeric) control the binding and release of cargo proteins. These interactions are controlled by a redox-sensitive amino acid, cysteine 10 of Pex5, which is essential for the formation of disulfide bond-linked Pex5 forms, for high affinity cargo binding, and for receptor recycling. Disulfide bond-linked Pex5 showed the highest affinity for PTS1 cargo. Upon reduction of the disulfide bond by dithiothreitol, Pex5 transitioned to a noncovalent dimer, concomitant with the partial release of PTS1 cargo. Additionally, dissipation of the redox balance between the cytosol and the peroxisome lumen caused an import defect. A hetero-oligomeric interaction between the N-terminal domain (amino acids 1–110) of Pex5 and a conserved motif at the C terminus of Pex8 further facilitates cargo release, but only under reducing conditions. This interaction is also important for the release of PTS1 proteins. We suggest a redox-regulated model for Pex5 function during the peroxisomal matrix protein import cycle.

Peroxisomes are organelles dedicated to lipid metabolism and scavenging of reactive oxygen species. The role of these intriguing organelles has recently been extended to aging, as well as to antiviral defense by activation of the rapid interferon-independent signaling pathway and/or stimulation of invariant natural killer T cells (1–4).

From yeast to plants and mammals, peroxisomes contain from several dozen to several hundred luminal proteins (5). Most peroxisomal matrix proteins contain a conserved C-terminal peroxisomal targeting signal 1 (PTS1),[3] which is comprised of a tripeptide, SKL, or its variants. The PTS1 receptor, Pex5, captures PTS1 proteins in the cytoplasm by a direct interaction between the C-terminal tetratricopeptide repeat (TPR) domains of Pex5 and the PTS1 motif of the cargo (6). The N-terminal disordered region (amino acids 1–276) of Pex5 is essential for interaction with other peroxins, such as Pex14 and Pex13, but is not required for its binding to canonical PTS1 proteins (7). In the absence of cargo, the TPR domains of Pex5 organize into an open, snail-like conformation and form a tunnel-shaped binding pocket. Upon binding of the PTS1 motif to the tunnel, the TPR domains transition to a closed, circular conformation (6). However, there are conflicting reports regarding the oligomeric states of Pex5 and the functions assigned to these states (8–11). Specifically, the mechanism and nature of the oligomeric species of Pex5 to which PTS1 proteins are bound are unclear.

The PTS1 receptor·cargo complex translocates across the peroxisomal membrane through an unusual protein channel, which opens up to 9 nm in diameter, and is composed of at least two proteins: Pex14 and the PTS1 receptor itself (12, 13). After unloading the peroxisomal cargo in the organelle lumen, Pex5 is exported by an unknown mechanism to the cytosolic side of the peroxisomal membrane, where it is monoubiquitinated on a conserved cysteine residue (Cys-10 in *Pichia pastoris* Pex5) near the N terminus (14, 15). The monoubiquitinated receptor is released to the cytosol by the action of AAA ATPases Pex1 and Pex6 for another round of import (16). When the receptor recycling pathway is blocked, Pex5 is polyubiquitinated at one (Lys-22 in *P. pastoris* Pex5) or two conserved N-terminal lysine residues and degraded by the proteasome (17). How the receptor recycling and degradation pathways are regulated is not known.

Unlike the endoplasmic reticulum, chloroplast and mitochondria, whose matrix protein import receptors are integral

* This work was supported, in whole or in part, by National Institutes of Health MERIT Award DK41737 (to S. S.).
[1] Present address: College of Life Sciences, Shandong Normal University, Jinan, Shandong, China, 250014.
[2] To whom correspondence should be addressed: Section of Molecular Biology, Div. of Biological Sciences, University of California, San Diego, Rm. 3326 Bonner Hall, 9500 Gilman Dr., La Jolla, CA 92093-0322. Tel.: 858-534-2327; Fax: 858-534-0053; E-mail: ssubramani@ucsd.edu.

[3] The abbreviations used are: PTS, peroxisomal targeting signal; dslPex5, disulfide bond-linked Pex5; ncPex5, noncovalent Pex5; NTD, N-terminal domain; RADAR, receptor accumulation and degradation in the absence of recycling; TPR, tetratricopeptide; Ni-NTA, nickel nitrilotriacetic acid.

TABLE 1
***P. pastoris* strains used in this study**

Name	Genotype	Reference
GS115	*his4*	Ref. 37
PPY12	*his4, arg4*	Ref. 38
PPY115	*his4, arg4, Δpex5 (ARG4)*	Ref. 39
SCM227	*his4, arg4, Δpex5 (ARG4) pAOX-BFP-SKL (ZEO)*	This study
SCM282	*his4, arg4, Δpex5 (ARG4) pAOX-BFP-SKL (ZEO) pPEX5-Pex5-HA (HIS4)*	This study
SCM284	*his4, arg4, Δpex5 (ARG4) pAOX-BFP-SKL (ZEO) pPEX5-Pex5-HA C10S (HIS4)*	This study
SCM286	*his4, arg4, Δpex5 (ARG4) pAOX-BFP-SKL (ZEO) pPEX5-Pex5-HA C338S (HIS4)*	This study
SCM288	*his4, arg4, Δpex5 (ARG4) pAOX-BFP-SKL (ZEO) pPEX5-Pex5-HA C444S (HIS4)*	This study
SCM290	*his4, arg4, Δpex5 (ARG4) pAOX-BFP-SKL (ZEO) pPEX5-Pex5-HA C338/444S (HIS4)*	This study
SCM301	*his4, arg4, Δpex5 (ARG4) pAOX-BFP-SKL (ZEO) pPEX5-Pex5-HA (HIS4) pPEX3-Pex3-mRFP (HPH)*	This study
SCM302	*his4, arg4, Δpex5 (ARG4) pAOX-BFP-SKL (ZEO) pPEX5-Pex5-HA (HIS4) pPEX3-Pex3-mRFP (HPH)*	This study
SCM303	*his4, arg4, Δpex5 (ARG4) pAOX-BFP-SKL (ZEO) pPEX5-Pex5-HA C10S (HIS4) pPEX3-Pex3-mRFP (HPH)*	This study
SCM304	*his4, arg4,* Δpex5 (ARG4) pAOX-BFP-SKL (ZEO) *pPEX5-Pex5-HA C338S* (HIS4) pPEX3-Pex3-mRFP (HPH)	This study
SCM305	*his4, arg4, Δpex5 (ARG4) pAOX-BFP-SKL (ZEO) pPEX5-Pex5-HA C444S (HIS4) pPEX3-Pex3-mRFP (HPH)*	This study
SCM306	*his4, arg4, Δpex5 (ARG4) pAOX-BFP-SKL (ZEO) pPEX5-Pex5-HA C338S/444S (HIS4) pPEX3-Pex3-mRFP (HPH)*	This study
SDH55	*his4, arg4, Δpex5 (ARG4) pAOX-BFP-SKL (ZEO) pPEX5-Pex5-HA C10S/K22R (HIS4) pPEX3-Pex3-mRFP (HPH)*	This study
JCR121	*his4, arg4, Δpex8 (ARG4)*	Ref. 27
SSGP01	*his4, arg4, Δpex8 (ARG4) Ppex8-Pex8(HIS)*	This study
SSGP02	*his4, arg4, Δpex8 (ARG4) Ppex8-Pex8ΔAKL(HIS)*	This study
SSGP03	*his4, arg4, Δpex8 (ARG4) Ppex8-Pex8Δ36 (HIS)*	This study
SSGP04	*his4, arg4, Δpex8 (ARG4) Ppex8-Pex8ΔWWYΔAKL (HIS)*	This study

membrane proteins, the peroxisomal receptor Pex5 and the PTS2 receptor Pex7 shuttle between the cytosol and the peroxisomal lumen (18, 19). Therefore, the peroxisomal receptors face a challenging problem because they must ensure high affinity binding to the PTS1 proteins in the cytosol but must not rebind them after their release in the peroxisomal lumen. How cargo is released is poorly understood. Pex8 from lower eukaryotic cells and Pex14 from higher eukaryotic cells have been suggested to be involved in the release of PTS1 proteins from Pex5, respectively (8, 20). However, the underlying molecular mechanism is not evident.

The redox state of the peroxisome lumen is more reducing than in the cytosol (21). Consistent with this observation, we show that the oligomeric states of Pex5 and their differential ability to bind cargo are under redox regulation. We identified Cys-10 in *P. pastoris* Pex5 as a redox-sensitive amino acid, which regulates the oligomeric state of Pex5, cargo binding, cargo release, and receptor recycling. We found that a disulfide bond-linked Pex5 (homo-oligomeric state) demonstrates the highest affinity for PTS1 cargo. Upon reduction of the disulfide bond *in vitro* by DTT, thereby mimicking the intraperoxisomal reducing environment, Pex5 transitions to a noncovalent dimer (homodimer) concomitantly with the partial release of PTS1 cargo. Dissipation of the redox balance between the cytosol and the peroxisome lumen with H_2O_2 causes a cargo import defect. The cargo release process is facilitated and driven to completion by the interaction between Pex5 and Pex8 (hetero-oligomeric state). We have identified the domains of Pex5 and Pex8 involved in this interaction, and we suggest a mechanistic model for Pex5 function during the import cycle for PTS1-containing proteins into the peroxisome matrix.

EXPERIMENTAL PROCEDURES

Yeast Strains, Plasmids, and Culture Conditions—The *P. pastoris* strains used are listed in Table 1. Growth medium components were as follows: rich medium YPD, 1% yeast extract, 2% peptone, 2% glucose; synthetic medium YNM, 0.67% yeast nitrogen base, 0.1% yeast extract, 0.5% (v/v) methanol; and mineral oleate medium YNO, 0.67% yeast nitrogen base, 0.1% yeast extract, 0.2% (v/v) oleate, 0.02% (v/v) Tween 40. Yeast cells were grown at 30 °C in YPD for 6–7 h, washed with distilled H_2O, and shifted either to synthetic methanol medium (YNM) or to mineral oleate medium (YNO) for biochemical experiments or fluorescence microscopy.

Plasmid Construction—The *PpPEX5* promoter was amplified and cloned into the pIB1 vector at SmaI-PstI sites, creating pCM256. The PpPEX5 ORF was amplified and transferred to pMY69 (lab stock) at ClaI-AflII sites to generate PpPex5 with a C-terminal HA tag. The Pex5-HA fragment was amplified and cloned downstream of the PpPEX5 promoter in pCM256 at PstI-HindIII sites, creating pCM259. Based on pCM259, the corresponding cysteine mutants (C10S, C338S, C444S, C338S/C444S, and C10S/K22R) were generated by site-directed mutagenesis. The pCM259 and the related cysteine mutant constructs were transformed into Δ*pex5*, which expresses a PTS1 cargo, BFP-SKL, from the alcohol oxidase promoter. For co-localization experiments, Pex3p-mRFP expressed from its own promoter was used.

P. pastoris Pex5 was amplified by PCR from genomic DNA and cloned in-frame at the AscI-HindIII sites into the pACYCDuet-1 vector (Novagen), generating pCM58. The corresponding Pex5 cysteine mutants (C10S, C338S, C444S, C338S/C444S, and N460K) and the truncated fragment (amino acids 1–110) were made by site-directed mutagenesis based on pCM58 and used for protein purification.

The *PpPEX8* promoter and ORF were amplified and cloned into the pIB1 vector between the KpnI-BamHI sites, creating pSGP01. Based on pSGP01, the corresponding mutants, Pex8Δ36, Pex8ΔAKL, and Pex8ΔWWYΔAKL, were generated by site-directed mutagenesis.

GFP with a N-terminal FLAG tag and a C-terminal PTS1 (SKL) was cloned into the pETDuet-1 vector (Novagen) at NcoI-NotI Sites, creating FLAG-GFP-SKL for co-purification with His-Pex5 or the pACYCDuet-1 vector at AscI-NotI, creating His-FLAG-GFP-SKL for estimation the size of GFP-SKL in the absence of receptor (used only in Fig. 4*C*).

Subcellular Fractionation and Protease Protection—Subcellular fractionation from oleate-induced yeast cells and the protease protection assay were performed as described previously (12).

Fluorescence Microscopy—Cells were grown in YPD medium and switched to YNM during exponential phase growth. Images were captured on a Zeiss Axioskop fluorescence microscope (AxioSkop 2 Plus, motorized) coupled to a cooled CCD monochrome camera (AxioCam MRM; Zeiss) and analyzed using AxioVision 4 software.

Protein Purification—The *P. pastoris* Pex5 and its cysteine mutants were expressed in *Escherichia coli*. Cultures were grown in LB medium to mid-log phase and induced by addition of 1 mm isopropyl-1-thio-β-D-galactopyranoside and incubated for 3 h at 30 °C. Cells were collected by centrifugation and resuspended in lysis buffer containing 50 mm NaH_2PO_4, 300 mm NaCl, 10 mM imidazole, 1 mM PMSF, Complete™ protease inhibitor (Roche Applied Science), and 1 mg/ml lysozyme. The cells were broken by sonication, followed by centrifugation to remove cell debris and other insoluble material. Supernatants were loaded onto a nickel-nitrilotriacetic acid (Ni-NTA) column (HisTrap FF column; GE Healthcare), and the proteins were purified using an AKTA purifier (GE Healthcare). To estimate the size of the recombinant His-Pex5 and His-Pex5 C10S, gel filtration analyses were performed on a gel filtration column (Superdex 200 10/300; GE Healthcare) equilibrated with buffer containing 50 mm NaH_2PO_4, 300 mm NaCl (pH 8.0). Fractions (250 μl) were collected and analyzed by SDS-PAGE, followed by Western blotting.

P. pastoris Pex8 with a C-terminal HA tag or Pex8Δ36 was amplified and transferred to pETM11 vector (a gift from Matthias Willmanns, EMBL, Germany), which contains a cleavable tobacco etch virus protease site after the His tag. The recombinant His-Pex8-HA and His-Pex8Δ36 were purified as described for His-Pex5, and their N-terminal His tag was cleaved by incubation with His tobacco etch virus protease overnight at 4 °C. The samples were incubated with Ni-NTA beads, and the supernatants were collected after centrifugation.

To generate His-Pex5·FLAG-GFP-SKL, proteins were co-expressed in *E. coli*. The complexes were first affinity-purified by HisTrap FF column, followed by gel filtration analysis using a gel filtration column (Hiload Superdex 200 16/60) in buffer containing 50 mM Tris (pH 8.0), 150 mM NaCl in the absence or presence of 10 mM DTT. Fractions (1 ml) were collected and analyzed by SDS-PAGE, followed by Protoblue staining or Western blotting.

GST Pulldown Assay—For assaying protein-protein interaction, ~1 μg of GST-SKL was immobilized on 20 μl of packed glutathione-Sepharose 4B slurry (GE Healthcare), incubated with whole cell lysates expressing equal amount of His-Pex5 or its relevant mutants in the binding buffer (50 mM NaH_2PO_4, 300 mM NaCl, 1 mm PMSF, Complete™ protease inhibitor; Roche Applied Science) for 2 h at 4 °C. The beads were washed five times with binding buffer. Bound proteins were analyzed by SDS-PAGE, followed by Western blotting with anti-His antibody.

Cargo Release Experiments—2 μg of His-Pex5·GFP-SKL complex was immobilized on 80 μl of Ni-NTA beads incubated overnight at 4 °C in binding buffer in the absence of DTT (50 mM NaH_2PO_4, 300 mM NaCl, 20 mM imidazole, 0.1% Triton X-100, and protease inhibitors). The beads were washed three times with binding buffer. The beads were aliquoted into four reactions and treated with or without 2 mM DTT or 4 μg each of Pex8-HA or Pex8Δ36 for 2 h at room temperature. Subsequently, the supernatants were aliquoted into fresh tubes and heated in sample buffer to 100 °C for 5 min. The beads were washed three times (50 mM NaH_2PO_4, 150 mM NaCl, 20 mM imidazole, 0.01% Triton X-100, and protease inhibitors) and eluted in sample buffer. Equal volumes of the supernatant and bead fractions were analyzed by SDS-PAGE, followed by Western blotting.

RESULTS

P. pastoris Pex5 Is Linked by Disulfide Bonds—To investigate whether Pex5 undergoes an oxidative modification, PpPex5 was TCA-precipitated from cells grown in methanol medium and analyzed using reducing and nonreducing SDS-PAGE. The anti-Pex5 antibody is specific because, under reducing conditions (+DTT), only a single band at ~72 kDa was detected in wild-type *P. pastoris,* but not in the Δ*pex5* strain (Fig. 1*A*, *left panel*). Under nonreducing SDS-PAGE (−DTT), in addition to the 72-kDa band, a band at ~140 kDa (corresponding to a Pex5 homodimer, see below) and two bands larger than 170 kDa (corresponding to Pex5 oligomers, see below) were observed (Fig. 1*A*, *right panel*). A band at ~80 kDa found upon SDS-PAGE in nonreducing conditions is likely the monoubiquitinated Pex5 (22). The high molecular mass Pex5 species visible by nonreducing SDS-PAGE were sensitive to 2 mM DTT and 2 mM GSH, indicating they are linked through disulfide bonds (Fig. 1*B*).

The high molecular mass species of PpPex5 found in *P. pastoris* could either be a homo- or a hetero-oligomeric complex with other peroxins or unknown proteins. Therefore, we expressed PpPex5 in *E. coli* to determine whether Pex5 can form a disulfide bond-linked dimer or oligomer. PpPex5 with an N-terminal His tag was first affinity-purified and then loaded onto a gel filtration column. During gel filtration chromatography, His-tagged PpPex5 appeared in two peaks as detected by anti-His antibody, corresponding to molecular masses of ~140 and ~280 kDa, respectively (Fig. 1*C*). In nonreducing gels, Pex5 in the 140-kDa peak ran as a single band (72 kDa), indicating that it is a noncovalent dimer. In contrast, Pex5 in the 280-kDa peak ran as two bands (140 and 72 kDa) of similar intensity, indicating that Pex5 in the 280-kDa peak is likely to be a tetramer composed of two homodimers linked by intermolecular disulfide bonds. We refer to the two forms of PpPex5 as disulfide bond-linked Pex5 (dslPex5) and noncovalent Pex5 (ncPex5), noting that different oligomeric states of Pex5 (monomer, dimer, or tetramer) have been reported based on the use of different organisms, buffers, and methods (9, 11, 23). When ncPex5 was concentrated in nondegassed buffer, approximately half of this species was converted to dslPex5 (Fig. 1*D*), corresponding to a similar band seen in the extracts of methanol-grown yeast cells (Fig. 1*A*, *right panel*).

The redox states between the cytosol and the intraperoxisomal matrix change when cells are grown in different media

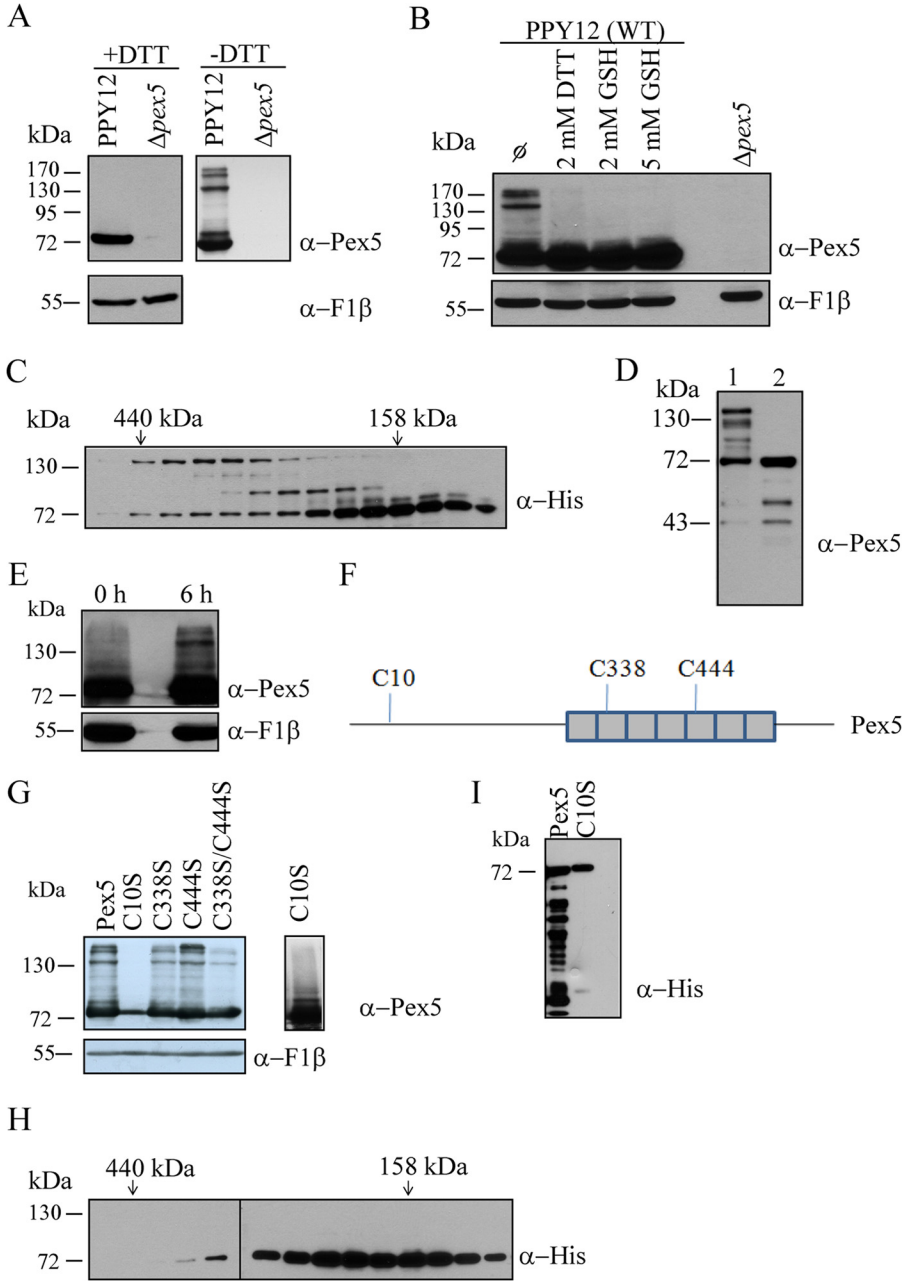

FIGURE 1. **Intermolecular disulfide bond-linked PpPex5 was found in *P. pastoris* and in *E. coli*.** *A*, cell lysates from wild-type (PPY12) and Δ*pex5* cells, grown overnight in methanol medium, were TCA-precipitated and separated by reducing (+DTT) or nonreducing (−DTT) SDS-PAGE, followed by immunoblotting with anti-Pex5 and anti-F1β (the loading control). *B*, cell lysates of wild-type cells from *A* were treated with reducing agents: 2 mM DTT, 2 mM GSH, or 5 mM GSH for 1 h at room temperature and analyzed by nonreducing SDS-PAGE, followed by immunoblotting with anti-Pex5 and anti-F1β. *C*, the affinity-purified recombinant His-Pex5 from *E. coli* was analyzed by gel filtration. The fractions collected were analyzed by nonreducing SDS-PAGE, followed by immunoblotting with anti-His antibodies. *D*, the noncovalent dimer of His-Pex5 purified from *E. coli* is oxidized to a covalent dimer. After gel filtration, the noncovalent dimer of Pex5 was concentrated and exchanged to a nondegassed buffer. The concentrated proteins treated without (*lane 1*) or with (*lane 2*) 2 mM DTT were analyzed by nonreducing SDS-PAGE, followed by immunoblotting with anti-His antibodies. The doublet of bands ~43 kDa (*lane 2*) was due to either degradation of full-length Pex5 or its truncated translation products. *E*, disulfide bond-linked PpPex5 was observed in *P. pastoris* under peroxisome proliferation conditions. *F*, PpPex5 contains three cysteines: Cys-10 located in the N-terminal domain and Cys-338 and Cys-444 located in the TPR domains. *G*, PpPex5 and its cysteine mutants were expressed from their own promoters in Δ*pex5* cells. Cell lysates of methanol grown cells were TCA-precipitated for nonreducing SDS-PAGE, followed by immunoblotting with anti-Pex5 and anti-F1β (*left panel*). The film was overexposed to show the absence of disulfide bond-linked Pex5 in Δ*pex5* cells transformed with PpPex5 C10S (*right panel*). *H*, the affinity-purified recombinant His-Pex5 C10S from *E. coli* was analyzed by gel filtration. The fractions collected were analyzed by nonreducing SDS-PAGE and immunoblotted with anti-His antibodies. *I*, wild-type Pex5 is more susceptible to proteolysis than is Pex5 C10S during expression and purification from *E. coli* cells.

(21). To investigate whether the dslPex5 correlates with the redox conditions under peroxisome proliferative conditions, Pex5 expressed from a constitutive GAPDH promoter was generated. The dslPex5 was barely discernible in rich glucose medium (Fig. 1*E*, *0 h*) but appeared when cells were grown in methanol medium (Fig. 1*E*, *6 h*). Therefore, the formation of dslPex5 was enhanced in peroxisome proliferation conditions.

PpPex5 Cys-10 Is Essential for the Formation of Disulfide Bond-linked Pex5—PpPex5 contains three cysteines, all of which are conserved among different Pex5 homologues.

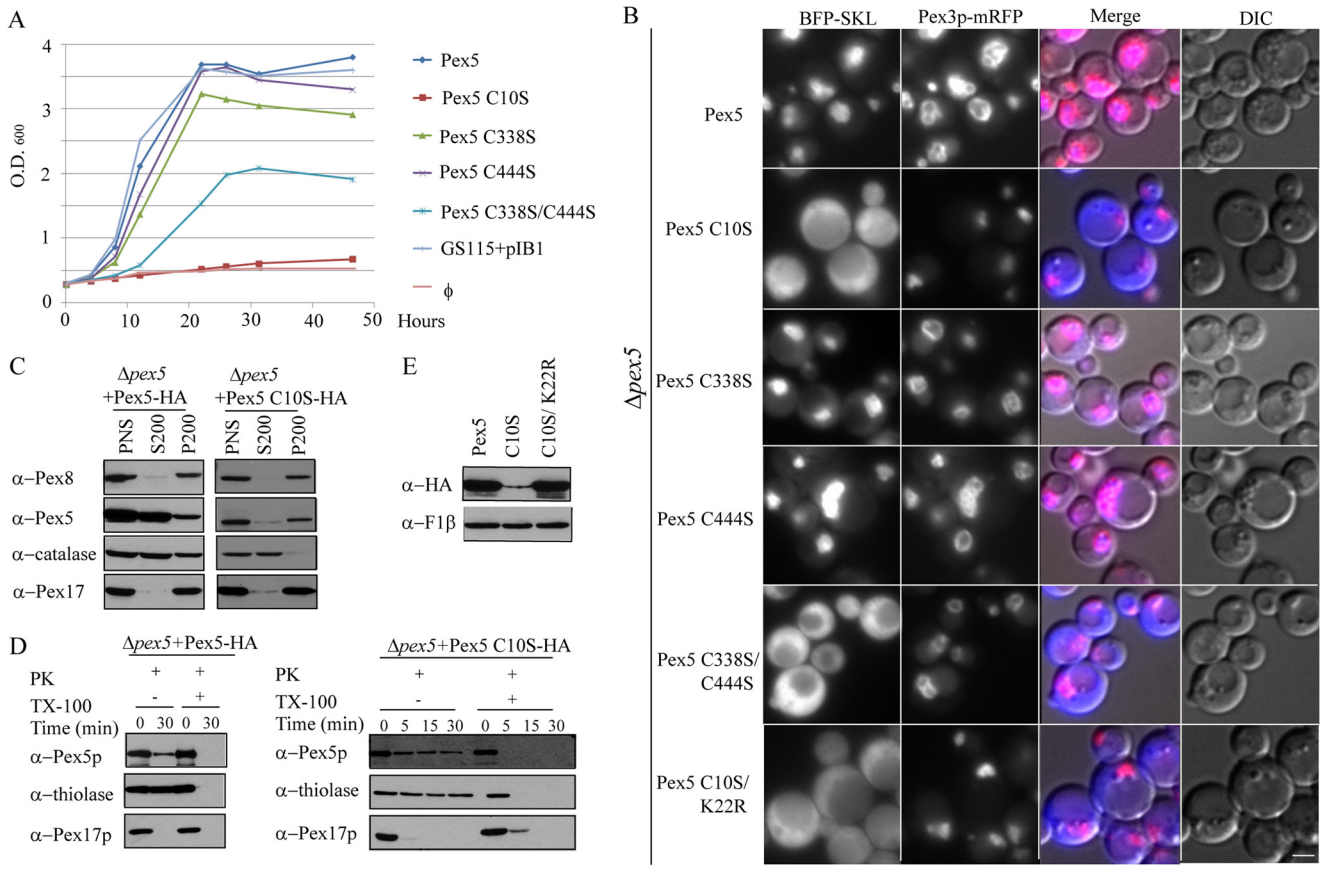

FIGURE 2. **The PpPex5 cysteine mutants have peroxisomal matrix protein import defects.** *A*, growth curve of cells in methanol medium. The Δ*pex5* cells harboring an overexpressed peroxisomal marker, BFP-SKL, were transformed with wild-type Pex5 or the relevant cysteine mutants expressed from the endogenous Pex5 promoter. The GS115 (*his4*) parent cells transformed with the pIB1 empty vector were used as a wild-type control. *B*, fluorescence microscopy analysis of Δ*pex5* cells expressing wild-type Pex5 or the relevant cysteine mutants from their endogeneous promoter. Pex3p-mRFP and BFP-SKL are peroxisomal membrane and matrix markers, respectively. *DIC*, differential interference contrast. *Scale bar*, 2 μm. *C*, differential centrifugation analysis. Equal proportions of 200,000 × *g* supernatant and pellet fractions from Δ*pex5* cells expressing wild-type Pex5 or Pex5 C10S were separated by SDS-PAGE and immunoblotted with the indicated antibodies. *D*, protease protection assay of a P200 pellet fraction isolated from Δ*pex5* cells expressing wild-type Pex5 or PpPex5 C10S. *E*, cell lysates from Δ*pex5* cells expressing wild-type PpPex5, PpPex5 C10S, and PpPex5 C10S/K22R were TCA-precipitated and separated by SDS-PAGE and immunoblotted with the indicated antibodies. *O.D.*, optical density; *PK*, proteinase K; *TX-100*, Triton X-100.

PpPex5 Cys-10 is located in the N-terminal disordered region, whereas Cys-338 and Cys-444 reside in the second and fifth TPR motif, respectively (Fig. 1*F*).

To investigate which cysteine(s) are required for the formation of dslPex5, the three cysteines were mutated to serine. The Pex5 cysteine mutants with a C-terminal HA tag, each expressed from their own promoters, were transformed independently into the Δ*pex5* strain. In contrast with wild-type PpPex5, the PpPex5 C10S mutant completely lost the ability to generate dslPex5 when induced in methanol medium overnight (Fig. 1*G*, *left panel*). However, when compared with wild-type Pex5, the expression level of PpPex5 C10S was low, but even in long exposures, we still did not see any dslPex5 (Fig. 1*G*, *right panel*). PpPex5 C338S and PpPex5 C444S did not show significant loss of dslPex5 (Fig. 1*G*, *left panel*). However, when both C338 and C444 were replaced by serine, the Pex5 bands above 170 kDa decreased significantly, suggesting that these two cysteines have a redundant role in the formation of intermolecular disulfide bond-linked Pex5 oligomers. Consistent with the *in vivo* data, *in vitro* purified PpPex5 C10S completely lost the disulfide bond-linked forms as well, and instead showed only the ncPex5 (Fig. 1*H*). When compared with wild-type Pex5, PpPex5 C10S may have a different conformation that is more resistant to the attack of proteases, because the affinity-purified Pex5 contained several degradation products that were almost nonexistent in the affinity-purified Pex5 C10S (Fig. 1*I*).

PpPex5 C10S Has a Defect in Importing Peroxisomal PTS1 Cargo—We reasoned that the three cysteines and the dslPex5 might be important for fulfilling the function of Pex5 as a PTS1 receptor. As shown by the growth curve in methanol medium, PpPex5 C10S did not complement Δ*pex5* cells (Fig. 2*A*). Although PpPex5 C338S and PpPex5 C444S eventually grew as well as the wild-type cells, both grew more slowly. Moreover, the PpPex5 C338S/C444S double mutant showed a more severe growth defect than the respective single mutants.

The inability of these Pex5 cysteine mutants to complement Δ*pex5* cells under peroxisome proliferation conditions indicates they may have a defect in importing PTS1 proteins into peroxisomes. Using fluorescence microscopy, we found that in Δ*pex5* cells complemented with wild-type Pex5 expressed from its own promoter, the peroxisomal PTS1 cargo, BFP-SKL, was targeted to punctate structures co-localizing with Pex3p-mRFP-labeled peroxisome clusters (Fig. 2*B*). However, in Δ*pex5* cells transformed with PpPex5 C10S, BFP-SKL was com-

pletely cytosolic. The targeting of BFP-SKL to peroxisomes was normal in Δ*pex5* cells transformed with either PpPex5 C338S or PpPex5 C444S. However, similar to the situation seen with PpPex5 C10S cells, BFP-SKL was predominantly cytosolic in the Pex5 C338S/C444S double mutant. These results indicate that the three cysteine residues of PpPex5 are important for its function as a PTS1 receptor and that Cys-338 and Cys-444 may perform redundant functions.

Disulfide Bond-free PpPex5 C10S Enters Peroxisomes and Is Degraded via the RADAR Pathway—To check whether the PpPex5 C10S mutant enters and exits peroxisomes, we performed differential centrifugation assays. As shown in Fig. 2*C*, in Δ*pex5* cells complemented with wild-type Pex5, the receptor was primarily in the cytosol fraction, whereas only a small amount was associated with the organelle fractions. Pex17, a peroxisomal membrane control, was associated with the organelle fractions, as expected. However, PpPex5 C10S was distributed more in the pellet than in the supernatant fraction, suggesting that it probably cannot be efficiently recycled. Moreover, consistent with the growth curve and fluorescence microscopy data, the peroxisomal import of catalase, a PTS1 cargo, was impaired in Δ*pex5* cells transformed with PpPex5 C10S.

To distinguish whether PpPex5 C10S entered the peroxisome lumen, we performed protease protection experiments (Fig. 2*D*). Similar to what was observed in the protease protection assay from the Δ*pex5* cells complemented with wild-type Pex5, PpPex5 C10S was resistant to protease treatment in the absence of detergent and was degraded only after the addition of Triton X-100. In contrast, Pex17 was susceptible to proteases even without detergent. However, thiolase, serving as a peroxisomal matrix protein control and targeted to the matrix in a Pex5-independent manner, was resistant to protease treatment in the absence of Triton.

The instability of PpPex5 C10S relative to wild-type Pex5 (Fig. 2*E*) suggests that it may be degraded by entering the RADAR pathway, because it cannot be monoubiquitinated on Cys-10 and recycled (22). If this hypothesis is true, mutating lysine 22, an amino acid predicted to be important for polyubiquitination on Pex5, should rescue the instability of PpPex5 C10S. Indeed, as shown in Fig. 2*E*, PpPex5 C10S/K22R was stabilized relative to PpPex5 C10S. However, stabilized Pex5 C10S/K22R could not rescue the import defects of Pex5 because of its inability to be recycled or degraded (Fig. 2*B*). Therefore, PpPex5 C10S can enter the peroxisome lumen and be transferred to the peroxisome membrane where it is degraded by the RADAR pathway.

Pex5 Cysteine Mutants Have Lower Binding Affinity for PTS1 Cargo—In contrast to PpPex5 C10S, PpPex20 C8S, which similarly blocks monoubiquitination and recycling of Pex20 showed only a mild growth defect, a result in line with the hypothesis that a deficiency in receptor recycling alone would result in a milder peroxisomal import defect, as long as the RADAR pathway is able to clear the receptor from the peroxisome membrane (24). The dysfunction of Pex5 C10S in peroxisome biogenesis could not be solely attributed to its instability. When Pex5 C10S was expressed from the GAPDH promoter in methanol medium for 3 h, it had a similar expression level as

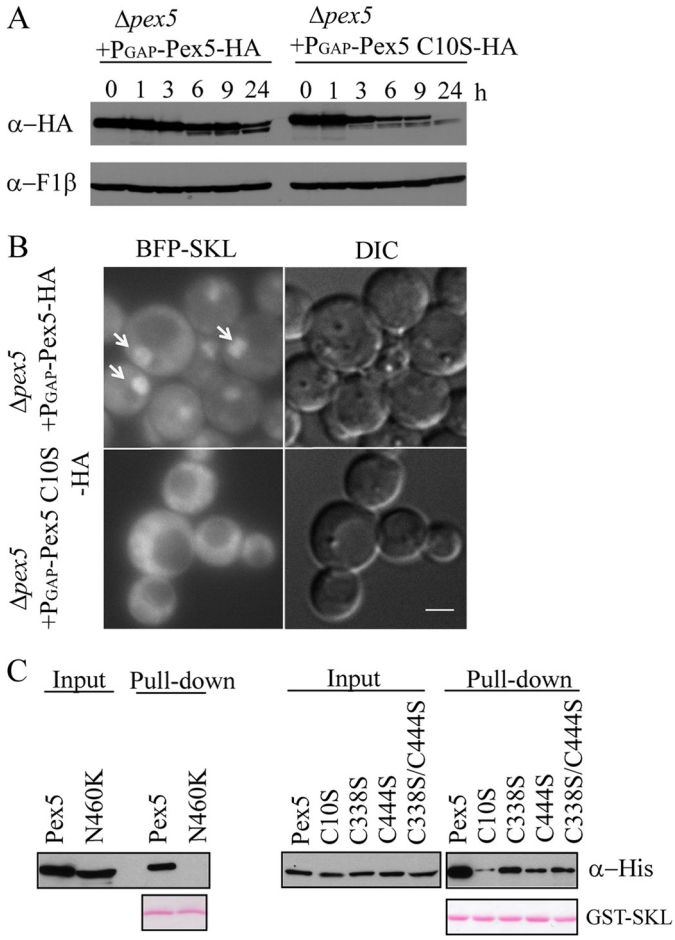

FIGURE 3. **PpPex5 C10S has a lower cargo binding affinity compared with wild-type Pex5.** *A*, the expression levels of Pex5 and Pex5C10S expressed from the GAPDH promoter in methanol medium were analyzed by Western blots. *B*, fluorescence microscopy analysis of Δ*pex5* cells co-expressing wild-type Pex5 or Pex5 C10S with BFP-SKL from the AOX promoter in methanol medium for 3 h. *Scale bar*, 2 μm. *C*, immobilized protein GST-SKL was incubated with *E. coli* cell lysates expressing PpPex5, C10S, C338S, C444S, C338/444S, or N460K mutants of PpPex5. After washing, bound proteins were eluted and analyzed by SDS-PAGE and Western blotted using anti-His antibodies. The GST-SKL was detected by Ponceau S staining. *DIC*, differential interference contrast.

WT Pex5 (Fig. 3*A*). However, BFP-SKL, expressed from the alcohol oxidase promoter, could only be imported efficiently in cells harboring a WT Pex5, but not Pex5 C10S (Fig. 3*B*). The severe PTS1 import defect observed in the PpPex5 C10S mutant suggests that PpPex5 Cys-10 may be involved in other steps in the peroxisomal matrix protein import cycle.

As a test of this hypothesis, the binding abilities of cargo to PpPex5 and PpPex5 C10S were tested by a GST pulldown assay. GST-SKL, a known peroxisomal matrix cargo, was bound to glutathione beads. Then cell lysates containing equal amounts of Pex5, or its cysteine mutants, were mixed with the beads to test their binding ability to the peroxisomal cargo in the absence of DTT. A Pex5 N460K mutant, which has been shown from different Pex5 homologues to be essential for cargo binding (25), was used as a negative control. As shown in Fig. 3*C*, PpPex5 C10S (*right panel*), similar to PpPex5 N460K (*left panel*), showed very low binding affinity to GST-SKL when compared with the wild-type Pex5. The other Pex5 cysteine

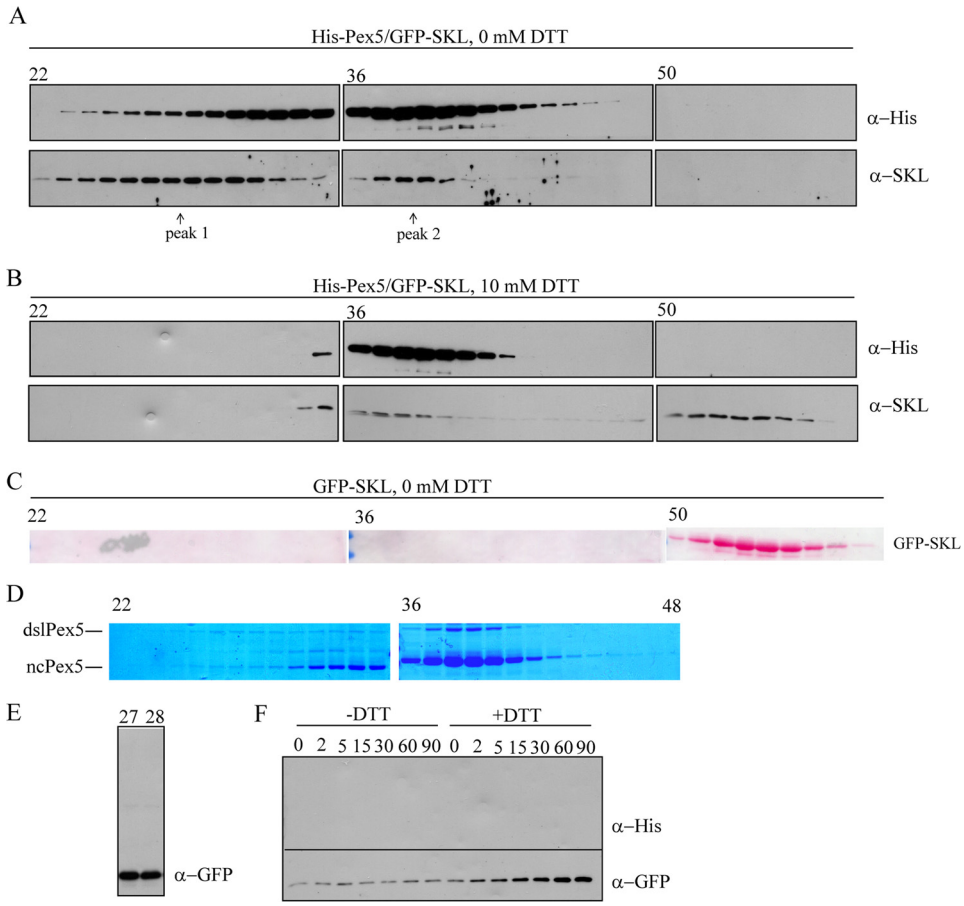

FIGURE 4. **Cargo release upon DTT treatment.** *A*, His-Pex5·GFP-SKL was co-expressed in *E. coli* and affinity-purified through a HisTrap FF column and then split into two aliquots: one was loaded onto a gel filtration column in buffer without DTT. *B*, the second aliquot was treated with 10 mM DTT for 1 h at room temperature and loaded onto a gel filtration column in buffer containing 10 mM DTT. The fractions were collected, separated by SDS-PAGE, and immunoblotted with the indicated antibodies. *C*, affinity-purified GFP-SKL was analyzed by gel filtration in the absence of DTT. The fractions were separated by SDS-PAGE, and the membrane was stained with Ponceau S. *D*, the affinity-purified His-Pex5·GFP-SKL complex was analyzed by gel filtration, and samples were collected for nonreducing SDS-PAGE (the same samples were used for reducing SDS-PAGE in *A* and stained by Protoblue (*A*) or immunoblotted with anti-GFP. *E*, the immunoblot was overexposed intentionally to confirm that there is no intermolecular disulfide linkage between Pex5 and GFP-SKL. *F*, His-Pex5·GFP-SKL complex was rebound to the Ni-NTA beads and incubated in the absence or presence of 1 mM DTT. At each time point, the beads were spun down, and the supernatant was collected and separated by SDS-PAGE to check the release of GFP-SKL from His-Pex5 by Western blot.

mutants had mildly reduced cargo binding affinities relative to wild-type Pex5.

PTS1 Cargo·Receptor Complex Dissociates upon DTT Treatment—To see whether reducing conditions play a role in cargo release, we first co-purified the His-Pex5·GFP-SKL complex under nonreducing conditions by affinity chromatography. Then we ran two separate gel filtrations, with and without 10 mM DTT. In the absence of DTT, GFP-SKL was mainly associated with dslPex5 in the first peak (Fig. 4, *A*, *fractions 23–33*, and *D*). A small portion of the GFP-SKL was associated with the second peak (Fig. 4*A*, *fractions 36–40*), which has a mixture of mostly noncovalent and some covalent dimers (Fig. 4*D*). However, the purified receptor·cargo complex was dissociated partially under reducing conditions (Fig. 4*B*). The dslPex5 was reduced to ncPex5 concomitant with the appearance of free GFP-SKL. Under reducing conditions, less than 50% of GFP-SKL was still associated with ncPex5. GFP-SKL itself is a monomer (Fig. 4*C*), and no intermolecular bond was found between Pex5 and GFP-SKL, as judged by the absence of this hetero-oligomeric species (Fig. 4*E*).

To see the kinetics of cargo release, the His-Pex5·GFP-SKL complex was first captured on Ni-NTA beads in the absence of reducing agents and then treated with or without 1 mM DTT for up to 90 min. In the presence of DTT, ~5-fold more cargo was released compared with treatment without DTT (Fig. 4*F*), indicating that the receptor·cargo complex dissociates under reducing conditions.

Dissipation of the Redox Balance between the Cytosol and the Peroxisome Lumen Causes an Import Defect—In glucose medium, the peroxisomal import machinery of wild-type cells was not sufficient to transport all GFP-SKL into peroxisomes when it was overexpressed from the GAPDH promoter. However, all the GFP-SKL was transported from the cytosol to peroxisomes after the cells were transferred from glucose medium to methanol medium for 3 h because there was no remaining cytosolic staining (Fig. 5*A*, *top panel*, compare *1 h* and *3 h*). In contrast, a significant amount of GFP-SKL remained in the cytosol when cells were exposed to 100 μM H_2O_2 for 3 h, indicating that maintaining a reducing peroxisomal lumen environment is important for cargo import (Fig. 5*A*, *lower*

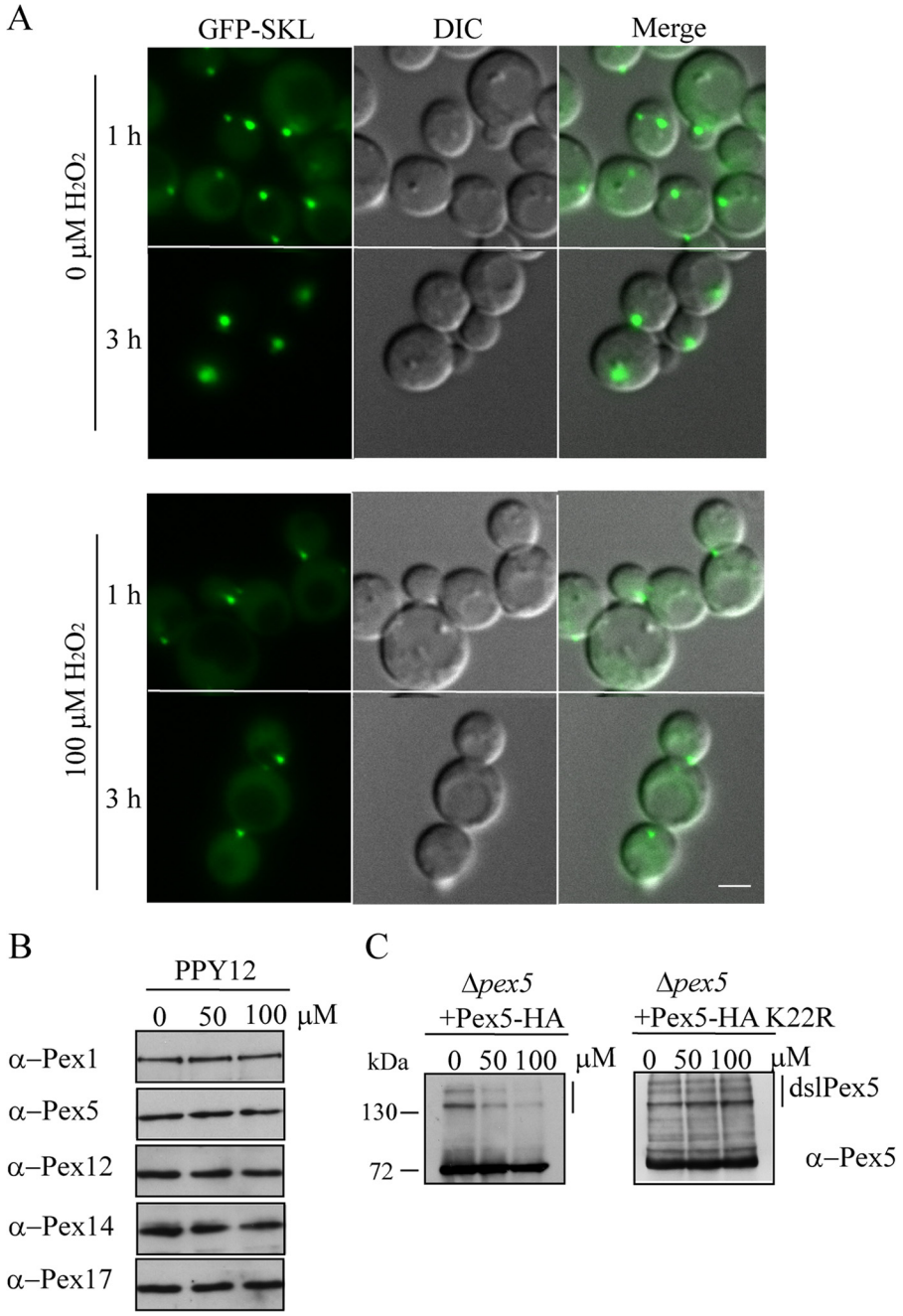

FIGURE 5. **Peroxisomal protein import was inhibited upon hydrogen peroxide treatment.** *A*, fluorescence microscopy analysis of methanol-grown wild-type cells expressing GFP-SKL from the GAPDH promoter. The cells were treated with H_2O_2 upon shift to the methanol medium. *Scale bar*, 2 μm. *B* and *C*, immunoblotting of cell lysates from methanol-grown cells used in *A* with the indicated antibodies. The cells were treated with 0, 50, or 100 μM H_2O_2. *C*, nonreducing SDS-PAGE followed by Western blot to analyze the expression level of dslPex5. *DIC*, differential interference contrast.

panel). The addition of 100 μM H_2O_2 caused a growth defect in methanol medium, but not in glucose or lactate medium, an indicator of functional mitochondria (data not shown). Moreover, the exposure of cells to 100 μM H_2O_2 did not significantly affect the expression of peroxins that are directly involved in peroxisomal matrix protein import (Fig. 5*B*). Surprisingly, we found less dslPex5 in cells treated with 100 μM H_2O_2 (Fig. 5*C*). This is likely caused by the activation of the RADAR pathway because, in the presence of 100 μM H_2O_2, the use of Pex5 K22R rescued the level of dslPex5 by blocking the RADAR pathway. These data are consistent with the hypothesis that oxidative stress impairs the recycling of Pex5.

Pex8 Facilitates Cargo Release—Next, we investigated whether PpPex8, an intraperoxisomal peroxin only found in yeast, has a role in mediating cargo release. PpPex8 contains a PTS1 but is fully functional in the absence of its PTS1 (26). Therefore, if Pex8 has any role in cargo release, it is unlikely to be executed by direct displacement of PTS1 cargo by binding of the PTS1 on Pex8 to the TPR domains of Pex5.

Zhang *et al.* (26) showed that Pex8 interacted, independently of its PTS1, with the N-terminal disordered region of Pex5. We further localized the binding region of Pex8 on Pex5 to the N-terminal 110 amino acids by using co-purification experiments (Fig. 6*A*).

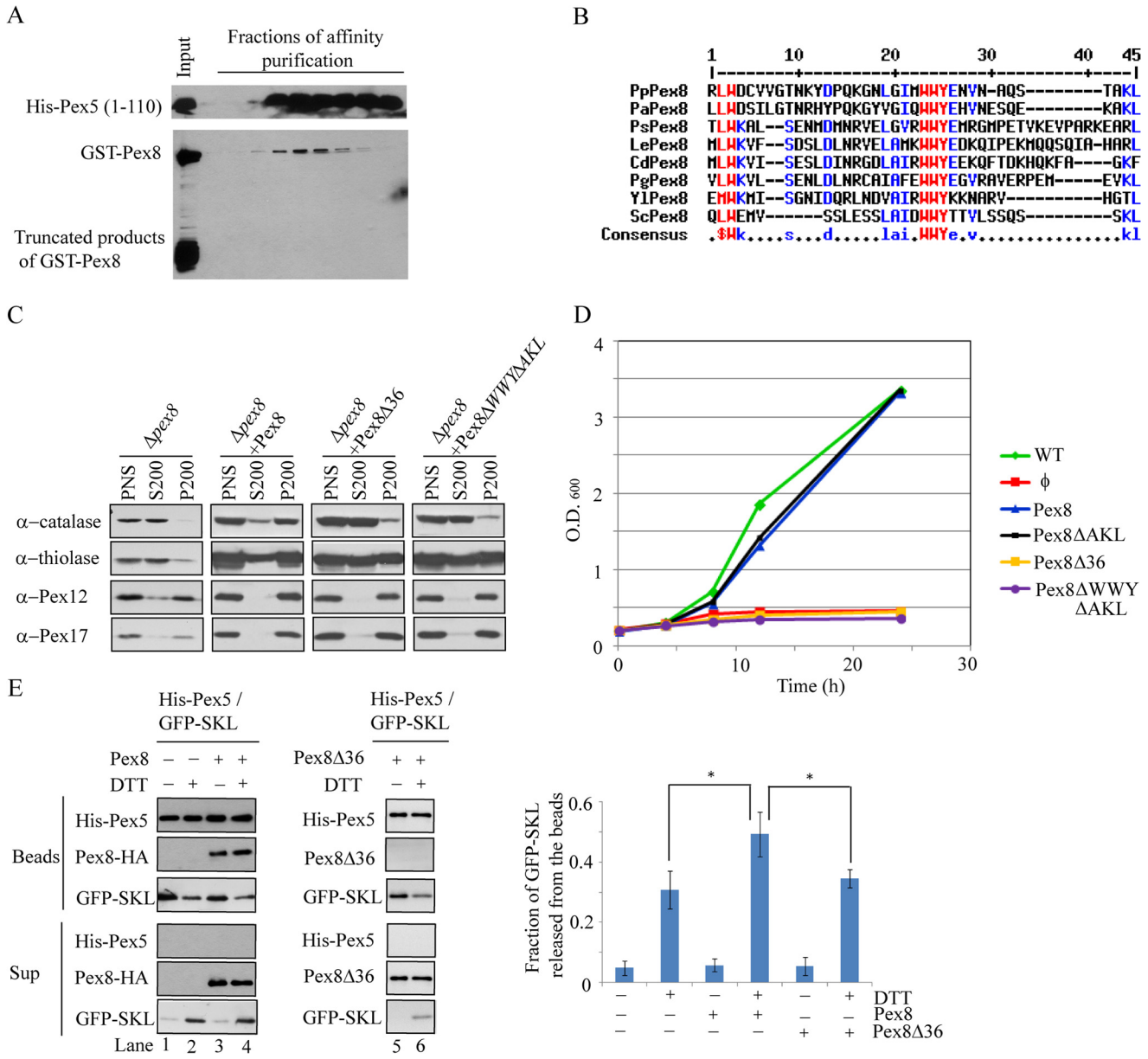

FIGURE 6. **Pex8 binds the NTD of Pex5 and facilitates the release of cargo.** *A*, co-purification of GST-Pex8 with His-Pex5 (1–110) via HisTrap FF column. GST-Pex8, but not the truncated products of GST-Pex8, is specifically co-purified with His-Pex5 (1–110). *B*, multisequence alignment of the C termini of Pex8 from *Candida dubliniensis* (*Cd*), *Lodderomyces elongisporus* (*Le*), *Phalaris angusta* (*Pa*), *Pichia guilliermondii* (*Pg*), *P. pastoris* (*Pp*), *Pichia stipitis* (*Ps*), *S. cerevisiae* (*Sc*), and *Yarrowia lipolytica* (*Yl*). *C*, differential centrifugation fractions from oleate-grown Δ*pex8* cells expressing Pex8, Pex8Δ36, or Pex8ΔWWYΔAKL were immunoblotted with the indicated antibodies. *D*, growth curve of WT, Δ*pex8*, and Δ*pex8* cells co-expressing Pex8 or the relevant Pex8 mutants in methanol medium. *E*, immobilized protein complex His-Pex5·GFP-SKL was incubated with Pex8 or Pex8Δ36 in the absence (−) or presence (+) of DTT. The beads were pelleted after 2 h, and the amounts of His-Pex5, GFP-SKL, and Pex8-HA in the supernatant and pellet were assessed (*left panel*). The bar graph on the *right* represents a quantification of the fraction of GFP-SKL released into the supernatant. The *error bar* represents the standard deviation of three independent experiments. * indicates a *p* value of <0.05 for the samples being compared. *O.D.*, optical density.

A *pex8* mutant, *per3-1*, described earlier appeared to efficiently import thiolase, a PTS2 protein, but was specifically impaired in the targeting of PTS1 proteins (21, 27), whereas in Δ*pex8* cells, both the PTS1 and PTS2 pathways were completely blocked. By sequencing the Pex8 locus of *per3-1*, we found that it lacks the last 36 amino acids of Pex8. A multisequence alignment indicates the existence of a short conserved motif (WWY) within the last 36 amino acids of Pex8 (Fig. 6*B*). When Pex8Δ36 was expressed from its own promoter in Δ*pex8* cells, the import of thiolase, but not catalase, was restored, confirming the importance of the C-terminal of Pex8 in the targeting of PTS1 proteins (Fig. 6*C*). Moreover, similar to Pex8Δ36, we found that Pex8ΔWWYΔAKL could selectively restore the PTS2, but not the PTS1, import pathway (Fig. 6*C*). Expression of neither Pex8Δ36 nor Pex8ΔWWYΔAKL could complement the growth defects of Δ*pex8* cells in methanol medium (Fig. 6*D*).

We investigated whether Pex8 could cause cargo release by the addition of an excess of recombinant Pex8 to the His-Pex5·FLAG-GFP-SKL complex, which was prebound to Ni-NTA beads in the absence of DTT. If Pex8 caused cargo release, one would expect GFP-SKL to be displaced into the supernatant. GFP-SKL was not released into the supernatant by disso-

ciation from Pex5 when incubated with Pex8 under nonreducing conditions (Fig. 6*E*, compare *GFP-SKL* in *Sup*, *lanes 1* and *3*, and *bar graph*). Thus, Pex8 on its own does not displace PTS1 proteins from the Pex5·cargo complex. However, more cargo was released upon addition of DTT and Pex8, but not Pex8Δ36, in comparison to the addition of DTT alone (Fig. 6*C*, compare *GFP-SKL* on beads and in *Sup*, *lanes 2*, *4*, and 6, and *bar graph*). Note that this difference in the behavior of Pex8 *versus* Pex8Δ36 is attributable to the ability of Pex5 in the beads fraction to bind Pex8, but not Pex8Δ36 (Fig. 6*E*, compare *lanes 3* and *4 versus lanes 5* and *6*). Therefore, whereas Pex8 does not directly cause PTS1 protein release from Pex5, it facilitates cargo release by interacting with the N-terminal domain of Pex5. In contrast, because Pex8Δ36 cannot bind Pex5, it fails to promote cargo release beyond the level caused by DTT alone (Fig. 6*E*, *bar graph*, *last column*).

DISCUSSION

In this manuscript we show that the formation and reduction of disulfide bonds via Cys-10 regulate the oligomeric state of Pex5, which allows PTS1 protein binding to, and release from, Pex5. Homo-oligomeric Pex5 linked by intermolecular disulfide bonds binds GFP-PTS1 cargo with the highest affinity and can be purified as a complex. Upon addition of DTT to reduce the disulfide bonds, thereby mimicking the reducing environment of the peroxisome matrix (21), Pex5 transitions to a noncovalent homodimeric form with a much lower affinity for PTS1 cargo, thereby resulting in partial cargo release. The subsequent hetero-oligomeric interaction between the N terminus of Pex5 with Pex8 shifts the equilibrium toward complete cargo release within the peroxisome. These studies provide insights into the molecular mechanism of cargo binding by Pex5 in the cytosol, shuttling to the peroxisome matrix where disulfide bond reduction and cargo release occur, and freeing up Cys-10, which is monoubiquitinated by Pex4, thereby allowing receptor export from the peroxisome membrane to the cytosol.

We show that dslPex5 accumulates under peroxisome proliferation conditions and can be reduced by 2 mM GSH. GSH is present in the peroxisomes of methylotrophic yeasts and is necessary for the metabolism of methanol (28) and known to be one of the important components involved in the plant peroxisomal ascorbate-glutathione cycle for scavenging reactive oxygen species (29). It is quite likely that GSH is also required to reduce the dslPex5 in the peroxisome lumen to facilitate cargo release and to make Cys-10 available for monoubiquitination. Failure to reduce the dslPex5 in the peroxisome lumen, or further oxidizing Cys-10 under oxidative stress conditions, may trigger an intracellular signal for polyubiquitination of Pex5, activating a quality control cascade whereby nonfunctional Pex5 is degraded through the RADAR pathway. This may be the true physiological reason for the existence and evolutionary conservation of the RADAR pathway, which is generally nonessential for peroxisome biogenesis, as long as receptor recycling is efficient. Consistent with this hypothesis, in the absence of *Hansenula polymorpha* PMP20, concomitant with the increase of oxidative stresses, the steady state level of HpPex5 was reduced when induced in methanol medium (30).

The C-terminal TPR domains of Pex5 are directly involved in cargo binding, whereas the N-terminal domain of Pex5 (NTD) contains motifs that interact with Pex14, Pex13, and Pex8. The NTD of Pex5 may also be involved directly or indirectly in modulating cargo binding. The role of the NTD in cargo binding could be explained by a direct interaction between the NTD and the TPR domains as suggested in mammalian Pex5: a competition between the PTS1 cargo and the NTD for binding to the TPR domain might result in the displacement of the PTS1 from the TPR domains (23). On the other hand, the reduction of the disulfide bond-linked NTD of Pex5 and the interaction between the NTD and other peroxins like Pex14 (20) and Pex8 (see below) may induce a conformational change in the C-terminal region of Pex5 corresponding to the TPR domains, which probably decreases the affinity to cargo and ultimately causes cargo release (6). We favor the second hypothesis because we did not see a significant interaction between the PpPex5 NTD and the TPR domains under reducing conditions (data not shown). The formation and disruption of the intermolecular disulfide bonds via Cys-10 may initiate an interdomain communication within Pex5 that regulates the affinity of cargo binding to, or release from, the TPR domains. Indeed, we found that the PpPex5 C10S mutant, which showed decreased binding capacity to cargo, may have a different conformation compared with PpPex5 because it is more resistant to proteases. It remains to be seen whether Pex14 interacts with the NTD of Pex5 in a manner that prevents disulfide bond formation, and in doing so, perhaps facilitates cargo release.

It has been suggested that Pex8 is involved in PTS1 protein release, but the molecular mechanism underlying this process is not known (8). Cargo release is not achieved by direct competition between Pex8 and PTS1 proteins in binding to the TPR domains of Pex5 because Pex8 can cause the PTS1 peptide to dissociate from Pex5 independent of its PTS1 (8). We found Pex8 binds to the N terminus of Pex5, which may induce a conformational change of the TPR domains and decrease their binding affinity to cargo. Furthermore, a conserved motif (WWY) at the C terminus of Pex8 was found to be essential for the targeting of PTS1 proteins. The binding of Pex8 to Pex5 in the peroxisome lumen makes the cargo release reaction irreversible and may further facilitate the subsequent receptor recycling process by maintaining the Cys-10 in its reduced state.

The intraperoxisomal redox state has been shown to be more reducing than that in the cytosol (21). Maintaining a reduced environment in the peroxisome lumen is crucial for Pex11-mediated peroxisome proliferation and the activity of peroxisomal 3-ketoacyl-CoA thiolase, an enzyme involved in fatty acid β-oxidation (31–33). Deletion of *Saccharomyces cerevisiae* glutathione peroxidase 1, an antioxidant using thioredoxin or glutathione for its reducing power, impaired peroxisome biogenesis (34). Knock-out of *PMP20*, a gene encoding a peroxiredoxin in *H. polymorpha*, impaired the targeting of peroxisomal matrix proteins, apparent consequences resulting from the reduced levels of Pex5 and phosphorylated Pex14 and damaged peroxisomal membranes. Legakis *et al.* (35) showed that peroxisomal PTS1 protein import is compromised in aging fibroblast cells, which produce an increased amount of reactive oxygen species.

Furthermore, they showed using an *in vitro* import assay that exposing early passage cells to 125 μM H_2O_2 significantly reduced the import of PTS1 protein. Although knock-out of genes encoding either glutathione peroxidase or PMP20 in *P. pastoris* showed neither a significant decline in PTS1-import (data not shown) nor reduced levels of Pex5, we found that exposing *P. pastoris* cells to 100 μM H_2O_2 caused a clear delay in the import of PTS1 proteins. Our studies indicate that intraperoxisomal reducing conditions are important for peroxisomal cargo import, *e.g.*, intraperoxisomal cargo release depends on reduced Pex5, a conformation that has a reduced binding affinity for cargo and a greater competence for undergoing monoubiquitination, fulfilling a necessary step for receptor recycling. Furthermore, the formation of dslPex5 through Cys-10 in the cytosol prevents irreversible oxidation, which reduces the binding ability of Pex5 to PTS1 proteins and subsequently activates the RADAR pathway.

How PTS2 cargo is released in peroxisome is still elusive. However, when a conserved cysteine (Cys-204) of Pex7 was mutated to serine or modified by NEM, the binding ability of Pex7 to the PTS2 cargo was significantly decreased (36). Whether Cys-204 is involved in PTS2 cargo releasing from Pex7 needs further investigation.

Acknowledgments—We thank the members of the Subramani lab for helpful discussion.

REFERENCES

1. Dixit, E., Boulant, S., Zhang, Y., Lee, A. S., Odendall, C., Shum, B., Hacohen, N., Chen, Z. J., Whelan, S. P., Fransen, M., Nibert, M. L., Superti-Furga, G., and Kagan, J. C. (2010) Peroxisomes are signaling platforms for antiviral innate immunity. *Cell* **141,** 668–681
2. Facciotti, F., Ramanjaneyulu, G. S., Lepore, M., Sansano, S., Cavallari, M., Kistowska, M., Forss-Petter, S., Ni, G., Colone, A., Singhal, A., Berger, J., Xia, C., Mori, L., and De Libero, G. (2012) Peroxisome-derived lipids are self antigens that stimulate invariant natural killer T cells in the thymus. *Nat. Immunol.* **13,** 474–480
3. Ma, C., Agrawal, G., and Subramani, S. (2011) Peroxisome assembly. Matrix and membrane protein biogenesis. *J. Cell Biol.* **193,** 7–16
4. Lanyon-Hogg, T., Warriner, S. L., and Baker, A. (2010) Getting a camel through the eye of a needle. The import of folded proteins by peroxisomes. *Biol. Cell* **102,** 245–263
5. Saleem, R. A., Smith, J. J., and Aitchison, J. D. (2006) Proteomics of the peroxisome. *Biochim. Biophys. Acta* **1763,** 1541–1551
6. Stanley, W. A., Filipp, F. V., Kursula, P., Schüller, N., Erdmann, R., Schliebs, W., Sattler, M., and Wilmanns, M. (2006) Recognition of a functional peroxisome type 1 target by the dynamic import receptor pex5p. *Mol. Cell* **24,** 653–663
7. Otera, H., Setoguchi, K., Hamasaki, M., Kumashiro, T., Shimizu, N., and Fujiki, Y. (2002) Peroxisomal targeting signal receptor Pex5p interacts with cargoes and import machinery components in a spatiotemporally differentiated manner. Conserved Pex5p W*XXX*F/Y motifs are critical for matrix protein import. *Mol. Cell. Biol.* **22,** 1639–1655
8. Wang, D., Visser, N. V., Veenhuis, M., and van der Klei, I. J. (2003) Physical interactions of the peroxisomal targeting signal 1 receptor pex5p, studied by fluorescence correlation spectroscopy. *J. Biol. Chem.* **278,** 43340–43345
9. Schliebs, W., Saidowsky, J., Agianian, B., Dodt, G., Herberg, F. W., and Kunau, W. H. (1999) Recombinant human peroxisomal targeting signal receptor PEX5. Structural basis for interaction of PEX5 with PEX14. *J. Biol. Chem.* **274,** 5666–5673
10. Madrid, K. P., De Crescenzo, G., Wang, S., and Jardim, A. (2004) Modulation of the *Leishmania donovani* peroxin 5 quaternary structure by peroxisomal targeting signal 1 ligands. *Mol. Cell. Biol.* **24,** 7331–7344
11. Costa-Rodrigues, J., Carvalho, A. F., Fransen, M., Hambruch, E., Schliebs, W., Sá-Miranda, C., and Azevedo, J. E. (2005) Pex5p, the peroxisomal cycling receptor, is a monomeric non-globular protein. *J. Biol. Chem.* **280,** 24404–24411
12. Ma, C., Schumann, U., Rayapuram, N., and Subramani, S. (2009) The peroxisomal matrix import of Pex8p requires only PTS receptors and Pex14p. *Mol. Biol. Cell* **20,** 3680–3689
13. Meinecke, M., Cizmowski, C., Schliebs, W., Krüger, V., Beck, S., Wagner, R., and Erdmann, R. (2010) The peroxisomal importomer constitutes a large and highly dynamic pore. *Nat Cell Biol.* **12,** 273–277
14. Platta, H. W., El Magraoui, F., Bäumer, B. E., Schlee, D., Girzalsky, W., and Erdmann, R. (2009) Pex2 and Pex12 function as protein-ubiquitin ligases in peroxisomal protein import. *Mol. Cell. Biol.* **29,** 5505–5516
15. Okumoto, K., Misono, S., Miyata, N., Matsumoto, Y., Mukai, S., and Fujiki, Y. (2011) Cysteine ubiquitination of PTS1 receptor Pex5p regulates Pex5p recycling. *Traffic* **12,** 1067–1083
16. Nashiro, C., Kashiwagi, A., Matsuzaki, T., Tamura, S., and Fujiki, Y. (2011) Recruiting mechanism of the AAA peroxins, Pex1p and Pex6p, to Pex26p on the peroxisomal membrane. *Traffic* **12,** 774–788
17. Platta, H. W., El Magraoui, F., Schlee, D., Grunau, S., Girzalsky, W., and Erdmann, R. (2007) Ubiquitination of the peroxisomal import receptor Pex5p is required for its recycling. *J. Cell Biol.* **177,** 197–204
18. Dammai, V., and Subramani, S. (2001) The human peroxisomal targeting signal receptor, Pex5p, is translocated into the peroxisomal matrix and recycled to the cytosol. *Cell* **105,** 187–196
19. Nair, D. M., Purdue, P. E., and Lazarow, P. B. (2004) Pex7p translocates in and out of peroxisomes in *Saccharomyces cerevisiae*. *J. Cell Biol.* **167,** 599–604
20. Freitas, M. O., Francisco, T., Rodrigues, T. A., Alencastre, I. S., Pinto, M. P., Grou, C. P., Carvalho, A. F., Fransen, M., Sá-Miranda, C., and Azevedo, J. E. (2011) PEX5 protein binds monomeric catalase blocking its tetramerization and releases it upon binding the N-terminal domain of PEX14. *J. Biol. Chem.* **286,** 40509–40519
21. Yano, T., Oku, M., Akeyama, N., Itoyama, A., Yurimoto, H., Kuge, S., Fujiki, Y., and Sakai, Y. (2010) A novel fluorescent sensor protein for visualization of redox states in the cytoplasm and in peroxisomes. *Mol. Cell. Biol.* **30,** 3758–3766
22. Liu, X., and Subramani, S. (2013) Unique requirements for mono- and polyubiquitination of the peroxisomal targeting signal co-receptor, Pex20. *J. Biol. Chem.* **288,** 7230–7240
23. Harano, T., Nose, S., Uezu, R., Shimizu, N., and Fujiki, Y. (2001) Hsp70 regulates the interaction between the peroxisome targeting signal type 1 (PTS1)-receptor Pex5p and PTS1. *Biochem. J.* **357,** 157–165
24. Léon, S., Zhang, L., McDonald, W. H., Yates, J., 3rd, Cregg, J. M., and Subramani, S. (2006) Dynamics of the peroxisomal import cycle of PpPex20p. Ubiquitin-dependent localization and regulation. *J. Cell Biol.* **172,** 67–78
25. Gatto, G. J., Jr., Geisbrecht, B. V., Gould, S. J., and Berg, J. M. (2000) Peroxisomal targeting signal-1 recognition by the TPR domains of human PEX5. *Nat. Struct. Biol.* **7,** 1091–1095
26. Zhang, L., Léon, S., and Subramani, S. (2006) Two independent pathways traffic the intraperoxisomal peroxin PpPex8p into peroxisomes. Mechanism and evolutionary implications. *Mol. Biol. Cell* **17,** 690–699
27. Liu, H., Tan, X., Russell, K. A., Veenhuis, M., and Cregg, J. M. (1995) PER3, a gene required for peroxisome biogenesis in *Pichia pastoris*, encodes a peroxisomal membrane protein involved in protein import. *J. Biol. Chem.* **270,** 10940–10951
28. Horiguchi, H., Yurimoto, H., Kato, N., and Sakai, Y. (2001) Antioxidant system within yeast peroxisome. Biochemical and physiological characterization of CbPmp20 in the methylotrophic yeast *Candida boidinii*. *J. Biol. Chem.* **276,** 14279–14288
29. Noctor, G., Queval, G., Mhamdi, A., Chaouch, S., and Foyer, C. H. (2011) Glutathione. *Arabidopsis Book* **9,** e0142
30. Bener Aksam, E., Jungwirth, H., Kohlwein, S. D., Ring, J., Madeo, F., Veenhuis, M., and van der Klei, I. J. (2008) Absence of the peroxiredoxin Pmp20 causes peroxisomal protein leakage and necrotic cell death. *Free Radic.*

Biol. Med. **45,** 1115–1124
31. Marshall, P. A., Dyer, J. M., Quick, M. E., and Goodman, J. M. (1996) Redox-sensitive homodimerization of Pex11p. A proposed mechanism to regulate peroxisomal division. *J. Cell Biol.* **135,** 123–137
32. Pye, V. E., Christensen, C. E., Dyer, J. H., Arent, S., and Henriksen, A. (2010) Peroxisomal plant 3-ketoacyl-CoA thiolase structure and activity are regulated by a sensitive redox switch. *J. Biol. Chem.* **285,** 24078–24088
33. Sundaramoorthy, R., Micossi, E., Alphey, M. S., Germain, V., Bryce, J. H., Smith, S. M., Leonard, G. A., and Hunter, W. N. (2006) The crystal structure of a plant 3-ketoacyl-CoA thiolase reveals the potential for redox control of peroxisomal fatty acid β-oxidation. *J. Mol. Biol.* **359,** 347–357
34. Ohdate, T., and Inoue, Y. (2012) Involvement of glutathione peroxidase 1 in growth and peroxisome formation in *Saccharomyces cerevisiae* in oleic acid medium. *Biochim. Biophys. Acta* **1821,** 1295–1305
35. Legakis, J. E., Koepke, J. I., Jedeszko, C., Barlaskar, F., Terlecky, L. J., Edwards, H. J., Walton, P. A., and Terlecky, S. R. (2002) Peroxisome senescence in human fibroblasts. *Mol. Biol. Cell* **13,** 4243–4255
36. Ghys, K., Fransen, M., Mannaerts, G. P., and Van Veldhoven, P. P. (2002) Functional studies on human Pex7p. Subcellular localization and interaction with proteins containing a peroxisome-targeting signal type 2 and other peroxins. *Biochem. J.* **365,** 41–50
37. Cregg, J. M., Barringer, K. J., Hessler, A. Y., and Madden, K. R. (1985) *Pichia pastoris* as a host system for transformations. *Mol. Cell. Biol.* **5,** 3376–3385
38. Gould, S. J., McCollum, D., Spong, A. P., Heyman, J. A., and Subramani, S. (1992) Development of the yeast *Pichia pastoris* as a model organism for a genetic and molecular analysis of peroxisome assembly. *Yeast* **8,** 613–628
39. McCollum, D., Monosov, E., and Subramani, S. (1993) The pas8 mutant of Pichia pastoris exhibits the peroxisomal protein import deficiencies of Zellweger syndrome cells. The PAS8 protein binds to the COOH-terminal tripeptide peroxisomal targeting signal, and is a member of the TPR protein family. *J. Cell Biol.* **121,** 761–774